Article:
Califano, M orcid.org/0000-0003-3199-3896 (2020) Charge Dynamics in Quantum-Dot–Acceptor Complexes in the Presence of Confining and Deconfining Ligands. Journal of Physical Chemistry Letters, 11 (1). pp. 280-285. ISSN 1948-7185

https://doi.org/10.1021/acs.jpclett.9b03073

Charge Dynamics in Quantum-Dot-Acceptor Complexes in the Presence of Confining and Deconfining Ligands

Marco Califano *

Pollard Institute, School of Electronic and Electrical Engineering, & Bragg Centre for Materials Research University of Leeds, Leeds LS2 9JT, United Kingdom

E-mail: m.califano@leeds.ac.uk

Abstract

Nanocrystal surface functionalization is becoming widespread for applications exploiting fast charge extraction or ultra-sensitive redox reactions. A variety of molecular acceptors are being linked to the dot surface via a new generation of organic ligands, ranging from neutral linkers to charge delocalizers. Understanding how core states interact with these molecular orbitals, localized outside the dot, is paramount for optimizing the design of efficient nanocrystal-acceptor conjugates. Here we look at two examples of this interaction: charge transfer to a molecular acceptor linked through either an exciton-delocalizing ligand or a more conventional localizing molecule. We find that such transfer can be described in terms of an Auger-mediated process whose rates can be tuned within a window of a few orders of magnitude (for the same dot-ligand-acceptor conjugate) by a suitable choice of the dispersion solvent and nanocrystal's dielectric environment. This result provides clear guidelines for charge extraction rate engineering in nanocrystal-based devices.

Graphical TOC Entry

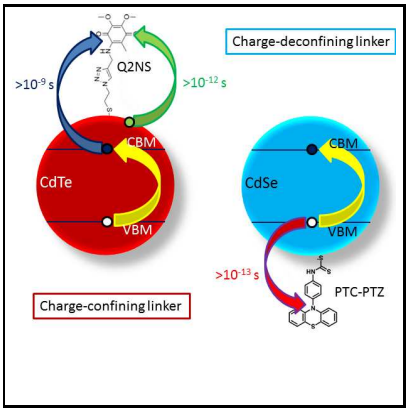

Semiconductor nanocrystals (NCs) owe their popularity to their simple and inexpensive synthesis and their size-tunable optical properties, which make them ideally suited for a wide range of applications.[1] While they are generally capped by organic ligands, chosen among a handful of possible alternatives, whose role is simply to passivate the surface dangling bonds, make them soluble and prevent aggregation, more recent applications, ranging from intracellular imaging of physical and biochemical parameters[2,3] and intercellular redox sensing,[4] to photon up-conversion[5] and energy harvesting, increasingly require the functionalisation of their surface with more specifically targeted molecules, whose role may include charge delocalization and/or linking to charge acceptors for redox reactions and efficient charge extraction. Indeed, Weiss' group recently reported[6] the observation of ultrafast (i.e., subpicosecond) hole transfer from a CdS colloidal quantum dot (CQD) to a molecular acceptor bound through a hole-delocalizing ligand to the dot surface. In order to optimise these systems' yield and better engineer their properties, it is however essential to understand what mechanism is responsible for the charge transfer between dot core and molecular acceptors and what factors can affect it.

Here we present an atomistic study of photoexcited hole and electron transfer from NC cores to molecular acceptors connected to the surface by either charge-delocalizing or charge-confining linkers. We find that good agreement can be obtained with experimentally measured charge transfer times by assuming an Auger-mediated transfer mechanism,[7] similar to that recently employed to explain the charge dynamics observed in CQDs of different materials and configurations, including CdSe cores,[8] InAs/ZnSe core/shell,[9] CdTe cores,[10] and impurity-doped CdSe:Te structures.[9]

First suggested by Frantsuzov and Marcus[7] as a possible explanation for blinking in CQDs, Auger-mediated transfer (AMT)[7–9] is a non-radiative decay process in which the transition energy of one charge carrier, e.g. the hole, moving from a core-delocalised state to an acceptor-localised state in the gap, is transferred to the photogenerated conduction band edge electron promoting it to another core-delocalised state at a higher energy (see

Fig. 1a). Equivalently, in the case of electron transfer to a molecular acceptor, the energy of the transition is transferred non-radiatively to the valence band, where a photogenerated hole is excited from the band edge to a deeper core-delocalised state (Fig. 1b and c).

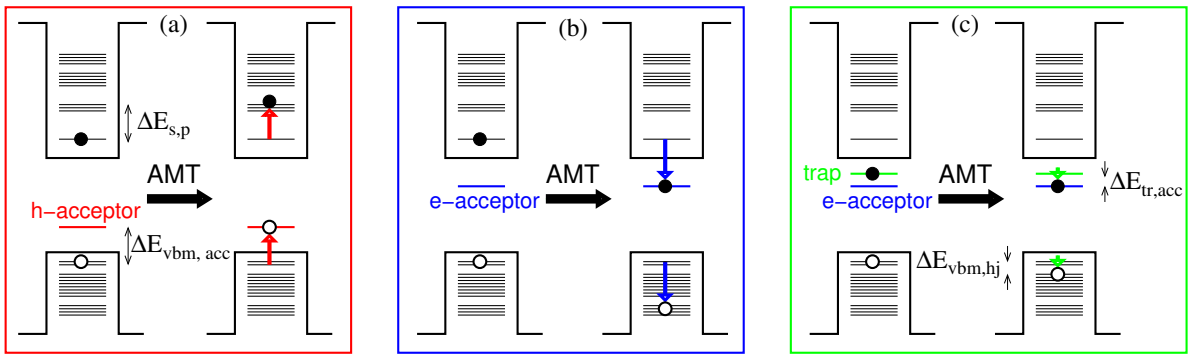

Figure 1: Schematics of the Auger-mediated transfer (AMT) mechanism considered in this work for both hole (panel a) and electron (panels b and c). In (a) and (b), the energy $\Delta E^{s,a}$ of the carrier transition $|s \rightarrow a_n>$ from the band edge s-like state to the intra-gap acceptor state a_n (n =h or el) is transferred non-radiatively to the oppositely charged carrier, also in an s-like core-delocalised band edge state, which is promoted into one of the excited core states j, situated $\Delta E^{s,j}$ higher in energy. Similarly, in (c) the energy $\Delta E^{t,a}$ of the carrier transition $|t \rightarrow a_n>$ from the trap state in the gap to the intra-gap acceptor state a_{el} is transferred non-radiatively to the VBM hole, which is promoted into one of the excited core states h_j, situated $\Delta E^{vbm,hj}$ higher in energy.

From its definition it should be apparent that an accurate description of this process is only possible within an atomistic approach, as the acceptor states involved exhibit typical localization lengths of the order of a few interatomic distances and are therefore beyond the reach of the popular $\mathbf{k}\cdot\mathbf{p}$ method. In this work the semiempirical pseudopotential method[11] - a state-of-the-art atomistic approach - is used.

Within the semi-empirical pseudopotential approach, the CQD is built with bulk-like structure, starting from its constituent atoms, up to the desired radius. This procedure yields surface atoms with unsaturated bonds. Atoms with only one (saturated) bond are removed, as they are unstable for dissociation,[12] leaving on the surface only atoms with one or two missing bonds. These surface dangling bonds are passivated by pseudo-hydrogenic, short-range potentials with Gaussian form.[13,14] A hole surface trap state was created by removing a single passivant from a surface anion. Electron surface trap states were modelled according

to the procedure detailed in Ref. [15]. The single-particle energies and wave functions were calculated using the plane-wave semiempirical pseudopotential method described in Ref. [11], including spin-orbit coupling, and excitonic effects were accounted for via a configuration interaction scheme.[16] (More detailed information on the theoretical method can be found in our previous work[8]).

AMT times were calculated using Fermi's Golden Rule according to[17]

$$(\tau_{\mathrm{AMT}})_i^{-1} = \frac{\Gamma}{\hbar} \sum_n \frac{| < i|\Delta H|f_n > |^2}{(E_{f_n} - E_i)^2 + (\Gamma/2)^2}. \quad (1)$$

where $|i>$ and $|f_n>$ are the initial and final excitonic states (see Fig. 1), E_i and E_{f_n} are their energies, ΔH is the Coulomb interaction and $\hbar/\Gamma$ is the lifetime of the final states.

Hole transfer to a molecular acceptor bound through a hole-delocalizing ligand: Our aim is to model hole transfer to an acceptor located not directly on the NC surface, but linked to it through a ligand that decreases the hole confinement and delocalizes its wave function. Indeed, ultrafast hole extraction was recently achieved with this configuration by Lian *et al.*[6] when linking phenothiazine (PTZ - a molecular hole acceptor) to a 2.0 nm-radius CQD through phenyldithiocarbamate (PTC), which they previously proved[18] to delocalize the hole wave function and lead to large bathochromic shifts, when coordinated to CdSe NCs.

We will therefore start by considering the linker: we model it as a simple atomic chain $\sim$ 1.1 nm long (consistent with the length of the real PTC[6]), made of a fictitious semiconductor material (suitably passivated by pseudo-hydrogen atoms), whose valence band edge lies above that of the NC, such that the highest occupied molecular orbital (HOMO) of the linker + acceptor complex has an energy of about -5.4 eV, as estimated by Lian *et al.*[6] for the PTC-PTZ complex.

A very detailed and accurate study of this QD-PTC conjugate system was recently carried out by Azpiroz and De Angelis,[19] who used *ab-initio* molecular dynamics and excited state

calculations to investigate the effects of the presence of aromatic dithiocarbamate molecules on the electronic and optical spectra of $Cd_{40}Se_{31}$ clusters. They did, however, not consider the effects of the presence of a molecular acceptor, like PTZ, nor calculate hole transfer rates to it. In what follows, we will show that, despite the simplicity of our ligand modelling, we can reproduce all the crucial features observed experimentally,[6,18] such as the bathochromic shifts, and predicted theoretically,[19] such as the character and localization of the carriers' wave functions.

Like in the actual case,[6,18] our model PTC (m-PTC) binds to Cd^{2+} sites on the NC surface. For simplicity, we assume monodentate anchoring, as the energy difference between the possible different anchoring geometries is small[20,21] and recent ab-initio calculations predicted[19] dithiocarbamate ligands to assume different anchoring geometries during the simulated trajectory. The latter also found the energy of the NC to be insensitive to the specific anchoring mode.

We investigate the effects on the electronic structure and optical properties of adding 1, 2, 4 and 48 linkers to a nearly spherical zincblende CdSe NC with $R = 1.2$ nm. As in the case of the *ab-initio* calculations by Azpiroz and De Angelis,[19] we find the emergence of 3 types of states (see Fig. 2): (i) core states, (ii) ligand states, and (iii) hybrid core-ligand states. Type (i) states include all conduction band minimum (CBM) states and the valence band maximum plus one (VBM+1) states for all NCs except the structure with 48 ligands; type (ii) include all gap states; whereas type (iii) states include all VBM states. We label states with over 50% of charge density localised on the surface as "linker" states. In contrast with Azpiroz and De Angelis, however, we label as CBM and VBM only states with over 50% of charge density localised in the core. This results in the appearance of linker states in the gap in our results, corresponding to the antibonding states at the top of the VB found by Azpiroz and De Angelis.

While the CBM is very little perturbed by the presence of the ligands up to a full coverage, the VBM shows signs of hybridization already with only 1 linker attached. The addition of

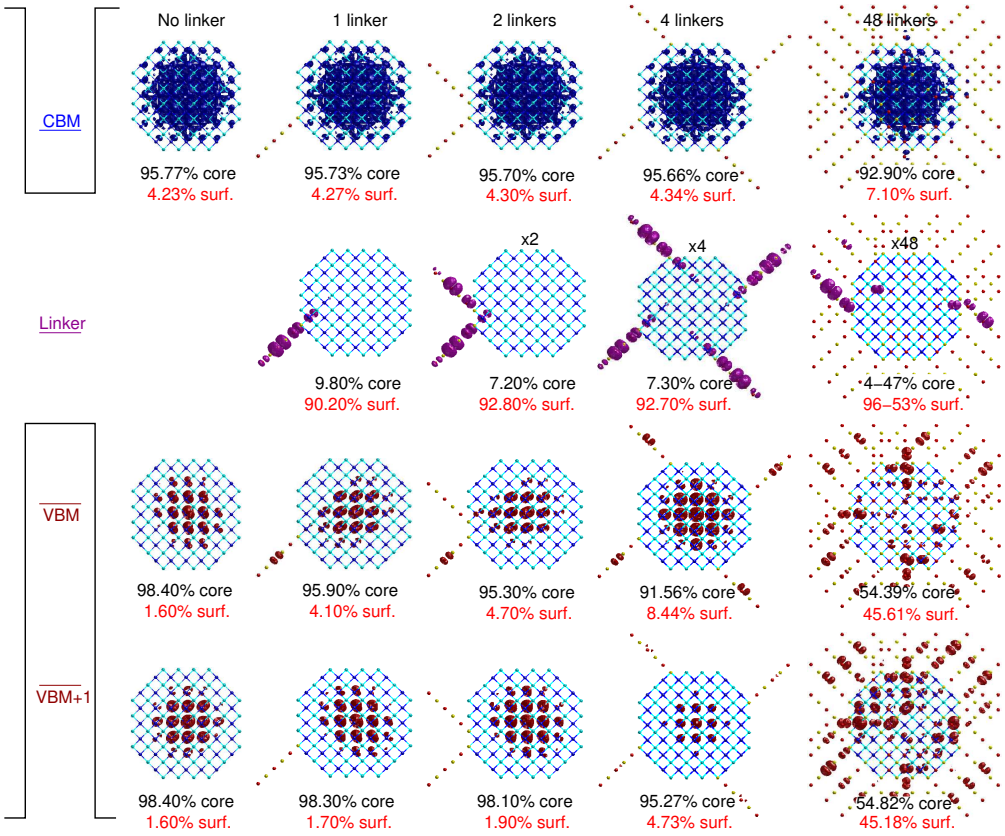

Figure 2: Calculated charge density distribution for cbm (blue, upper panels), linker states (magenta, middle panels), and vbm and vbm+1 (red, lower panels), superimposed onto the atomic structure of NC and linker, together with the percentage of localization within the dot core (black figures) and on the surface (red figures). Although the number of linker states in the gap equals the number of ligands on the surface, the charge density of only one representative linker state is shown for each ligand configuration. A cartoon of the electronic structure showing the relevant energy level (not to scale) is also shown on the left.

further ligands progressively increases this effect, leading to a proportional reduction of the VBM's wave function localization in the core to about 54% with 48 ligands. This is not the case for the next (VBM+1) valence band state, which is nearly unaffected by the addition of up to 4 ligands, as confirmed by the very small variation of its calculated charge density in the core. When the surface is saturated with linkers, however, its wave function localization closely resembles that of the VBM. (For configurations with up to four ligands on the surface, all linker states are nearly identical; hence only one representative state, randomly selected, is shown in Fig. 2. This is not the case with 48 ligands, when the linker states may exhibit very different charge localizations on the surface, varying from 53% to 96%). In contrast, in the presence of a hole non-delocalizing (HND) ligand (the charge densities relative to a configuration with four such ligands is compared with those obtained in the presence of four m-PTC in Fig. S1, Supporting Information), which we model as an atomic chain identical to our m-PTC, but made of a material with a VBM positioned well below that of the NC, we find no linker states in the gap, no hybrid states close to the band edges and nearly perfectly confined CBM and VBM.

This behaviour confirms therefore that our m-PTC exhibits the characteristics expected of a hole-delocalizing ligand. The comparison between calculated and observed band edge energy shifts (Fig. 3) further proves that our model CQD-ligand system quantitatively reproduces the deconfinement measured in experimental CdSe-PTC conjugates of similar size. In contrast, the prediction by Azpiroz and De Angelis[19] (empty red symbol in Fig. 3), clearly underestimates the shift.

Having established the credibility of our model ligand through its accurate prediction of PTC's hole-deconfining effects, we can now proceed to the next step: the creation of a hole acceptor. As mentioned previously, the main characteristic we aim to reproduce is the position of the PTC-PTZ HOMO energy, as the efficiency of the hole transfer will be crucially affected by the relative position of the NC's VBM and the HOMO of the PTC-PTZ system. The acceptor state is obtained by unpassivating one of the dangling bonds of the end atom

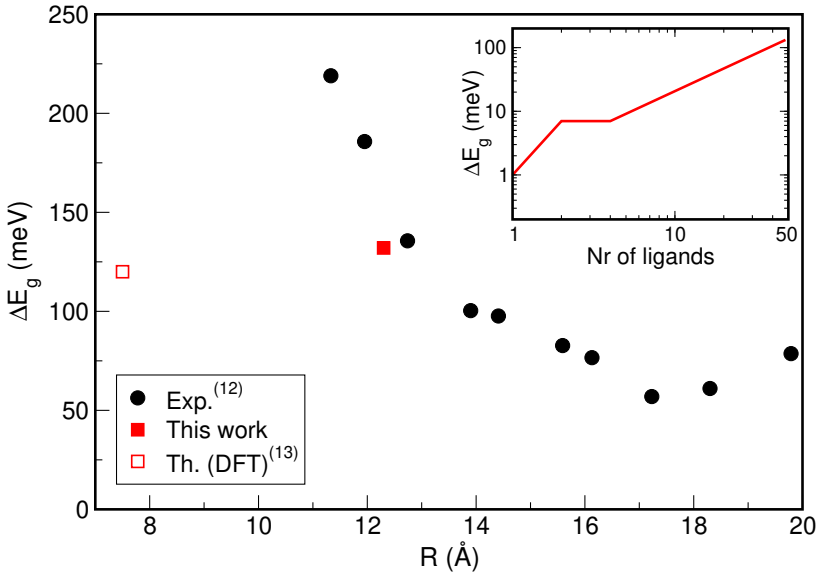

Figure 3: Main panel: energy shift as a function of the NC radius: comparison between theory (this work, solid red square) and experiment.[18] The result of the *ab-initio* calculations by Azpiroz and De Angelis[19] is also shown for comparison (empty red square). Inset: Calculated energy shift as a function of the number of ligands present on the NC surface.

(anion) of our m-PTC. This creates a state in the gap 5.44 eV below the vacuum level, which is in good agreement with the energy position of the PTC-PTZ (-5.38 eV) measured by cyclic voltammetry,[6] further confirming the suitability of our choice of the linker material.

The calculated Auger-mediated transfer times to such an acceptor state in different dielectric environments are displayed in Fig. 4 as a function of ΔE, the variation of the energy position of the linker-acceptor HOMO with respect to its calculated value (-5.44 eV, corresponding to $\Delta E = 0$). These variations in the acceptor depth may originate from size/shape anisotropy in the sample and/or external causes (such as local electric fields), but may also account for inaccuracies in the exact theoretical determination of this quantity compared to experiment ($\Delta E^{\text{th-exp}}_{\text{HOMO}} = E^{\text{exp}}_{\text{HOMO}} - E^{\text{th}}_{\text{HOMO}} \sim 0.06$ eV in the present case). We find the AMT rates to be especially sensitive to two main parameters: the energetic position of the acceptor state with respect to the VBM (i.e., the acceptor depth), and the dielectric environment of the CQD-acceptor conjugate. Our results show that the hole transfer time can be as fast as ~ 100 fs, falling below the experimental resolution - 300 fs (black dashed line in Fig. 4) - available to Lian *et al.*,[6] in the presence of a *single* linker-acceptor system

on the whole NC surface, for all values of the external dielectric constant ϵ_{out} considered (as all transient absorption spectra taken by Lian and co-workers were obtained on samples dispersed in benzene-d_6,[6] we only considered values for the dielectric constant close to ϵ(benzene) - i.e., ~ 2.2 - which also cover most common ligands and solvents), for ΔE in selected intervals. However, for any specific value of ΔE, the transfer times vary by a few orders of magnitude, depending on the dielectric environment, e.g. $\tau_{\Delta E=0} = 0.219$ ps for $\epsilon_{\text{out}} = 2.0$ and $\tau_{\Delta E=0} = 21.829$ ps for $\epsilon_{\text{out}} = 2.5$.

A similar behavior is also found when increasing the number of linker-acceptor complexes on the NC surface (see Fig. S2, Supporting Information), with the fastest hole transfers still taking place on sub-300 fs times, and a slight shift of the curves' minima towards higher values of ΔE. Figure S2 shows that by shifting the calculated position of the HOMO of our m-PTC/m-PTZ complex by 0.06 eV (i.e., for $\Delta E = 0.06$ eV) the predicted hole transfer time in our NC-acceptor conjugate dispersed in benzene ($\epsilon_{\text{out}} = 2.2$) is in excellent agreement with experiment. Interestingly this shift corresponds to the discrepancy between theoretical and experimental estimates for the PTC-PTZ HOMO, i.e., the value of $\Delta E^{\text{th-exp}}_{\text{HOMO}}$ discussed above.

These results show that, although in order to reproduce the bathochromic shifts observed experimentally,[18] the PTC molecules need to cover the entire NC surface, efficient, sub-picosecond hole transfer to PTZ is achievable in the presence of a single linker-acceptor complex, owing to the hole-deconfining effect of PTC, which leads to a strong coupling between core and acceptor states, through hybridised wave functions.

They also indicate that the dielectric environment of the CQD-acceptor conjugate (i.e., the solvent in which the nanostructures are dispersed) can be used as a mean by which the hole transfer time can be further fine tuned within a window of a few orders of magnitude, for the same choice of linker-acceptor complex. On the other hand, the transfer time can also be engineered by modifying the depth of the linker-acceptor HOMO, through the introduction of, e.g., NC shape distortions (elongations) or local electric fields.

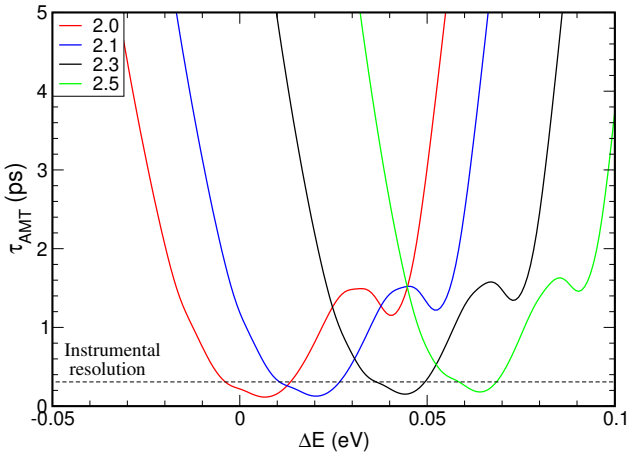

Figure 4: Calculated Auger-mediated hole transfer times to a single linker-acceptor complex, as a function of the variation of the energy position of the linker-acceptor HOMO with respect to its calculated value (-5.44 eV, $\Delta E = 0$), for different values of the dielectric constant of the NC-acceptor conjugate's environment, from 2 (red curve) to 2.5 (green curve), covering common ligands and solvents. Experimental transfer times were obtained for samples dispersed in benzene (ϵ(benzene)=2-2.3, depending on temperature). The instrumental resolution limit in [6] is marked by a horizontal dashed line.

Electron transfer to a molecular acceptor bound through an electron non-delocalizing ligand: Here we consider the case of a CdTe CQD conjugated with a quinone molecule (Q2NS, an electron acceptor based on the structure of the metabolic cofactor coenzyme Q_{10}), which has been recently proposed[4] as a highly-sensitive fluorimetric redox sensor for applications ranging from chemical detection to bioimaging. As in the case of PTC, we model the linker as a one-atom-thick arm made of a semiconductor material, whose length (0.70 nm) is based on that estimated for the real molecule (704 ± 6 pm).[4] Unlike for our m-PTC, however, in order to reproduce the experimental conditions,[4] its band gap was engineered to be much greater than that of the NC material, resulting in the absence of any states in the gap and of any electronic coupling between NC and acceptor through the linker (Fig. S3 Supporting Information).

Finally, the Q2NS is modelled as a localized acceptor state positioned at the end of the linker, specifically engineered so that its energetic position (-4.73 eV, with respect to vacuum) reproduces the experimentally estimated position[4] of the lowest unoccupied molecular orbital (LUMO) of Q2NS, obtained from cyclic voltammetry data (-4.81± 0.09 eV).

The calculated electron transfer times to such an acceptor from a core-delocalized state in a nearly spherical, zincblende CdTe NC with $R = 1.45$ nm, exceed 1 ns (Fig. S4 Supporting Information) for different positions of the linker on the NC surface and of the acceptor on the linker end group. In contrast, electron transfer times up to 3 orders of magnitude faster were recently calculated[15] for transitions to molecular acceptors (methylene blue) adsorbed directly onto the surface of CdSe NCs with radii between 1 and 1.9 nm (similar times were also observed (i) for transfers to methyl viologen, and anthraquinone and (ii) in CdS and CdTe NCs[15] of similar sizes). Such a large difference is due to the very different degree of electronic coupling taking place between the core-delocalized state and the acceptor-localized state in the two configurations. In the case of the CdTe-Q2NS structure, however, transfer times in the ps range were extracted experimentally from population decay curves, despite the large distance (and poor coupling) existing between core and acceptor. This efficient transfer was attributed to a surface-trap-mediated Auger mechanism (Fig. 1c), in which the enhanced coupling between a surface-trapped electron and an acceptor located close to the trap could account for the fast transfer time.

Figure 5 shows the transfer times calculated in this scenario for different trap-acceptor separations. We find orders of magnitude variations in the transfer times, ranging from a few ps, when trap and acceptor are close, to tens of ns, when they are on opposite sides of the NC. Unlike in the case of the hole transfer to PTC/PTZ, however, the effect of the dielectric environment is very weak here (the largest difference we find in the transfer times is less than a factor of 10 - obtained for the slowest transfers - when varying ϵ_{out} from 2.2 to 8.5), as in this case both initial and final electronic states are either on or outside the surface and therefore experience the same external environment. Also the qualitative behavior of the transfer times vs ΔE is different in the two cases (see Fig. S5, Supporting Information): while in the case of the hole transfer (Fig. 4 and Fig. S2, Supporting Information), the depth of the acceptor $\Delta E_{\mathrm{vbm,acc}} = E_{\mathrm{acc}} - E_{\mathrm{vbm}}$ (see Fig. 1a) had to match the s-p splitting in the conduction band $\Delta E_{sp} = E_p - E_{\mathrm{cbm}}$ (i.e. the energetic separation between s-like CBM and the p-like

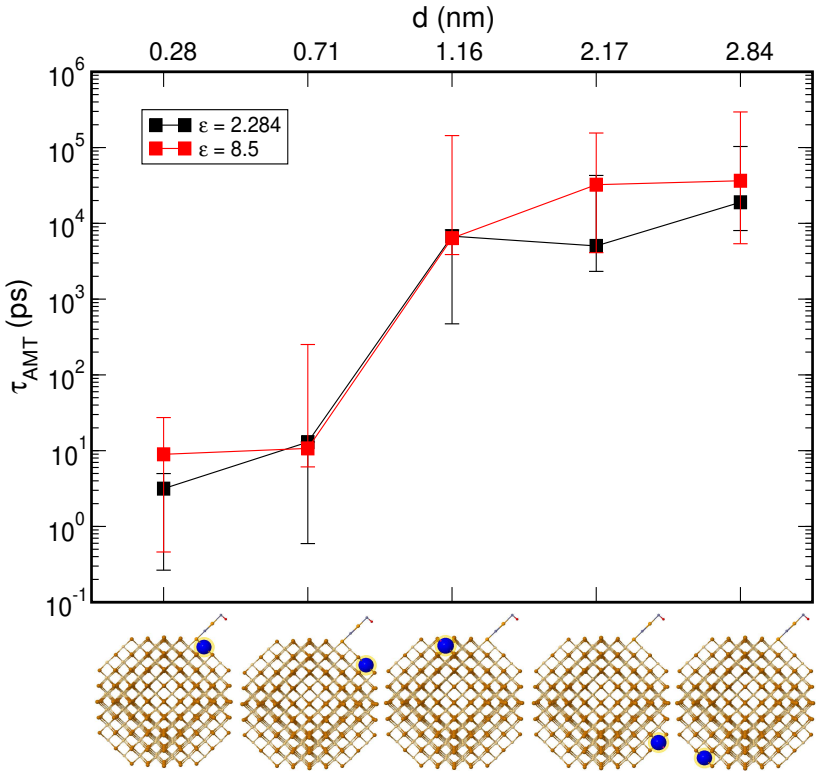

Figure 5: Auger-mediated electron transfer times from a surface trap to a single linker-acceptor complex, calculated as a function of the separation between trap and linker anchor group (top x axis - not to scale), for different values of the dielectric constant of the NC-acceptor conjugate's environment, from 2.284 (black symbols) to 8.5 (red symbols), covering common ligands, solvents and shell materials. The position of the surface trap is indicated by the blue sphere (whose dimensions are exaggerated for clarity) in the atomistic structure cartoons on the bottom x axis. The error bars are obtained as explained in Fig. S5, Supporting Information.

higher states) in order for energy to be conserved in the transition, resulting in a curve with a very narrow dip, in the case of electron transfer (see Fig. S5, Supporting Information), due to the denser energy spectrum of the valence band it is much more likely that an excited hole state will be found whose separation from the VBM, $\Delta E_{\mathrm{vbm},h_j} = E_{\mathrm{vbm}} - E_{h_j}$ matches the energy difference between trap and acceptor $\Delta E_{\mathrm{tr,acc}}$ (see Fig. 1c), for any value of this difference, hence the more oscillating character of the curve, that exhibits several minima corresponding to all possible resonances $\Delta E_{\mathrm{vbm},h_j}$ for transitions $|vbm\rangle \rightarrow |h_j\rangle$ in the VB.

Indeed, the expression for the trapping rate Eq. (1) can be separated into AMT coupling (numerator) and energy conservation (denominator): the matrix elements relative to AMT transitions in the two configurations (the numerator of Eq. (1)) can be very similar, for the case of the closest trap. This can be seen from the fact that the minima of the τ_{AMT} vs ΔE curves are close to 100 fs for both hole and electron transfers (compare any curve in Fig. 4 with the blue curve in Fig. S5, Supporting Information).

These results show that, in the presence of a non-deconfining linker, efficient charge transfer to the acceptor requires a trap-mediated process. Furthermore, as the transfer time depends crucially on the distance between trap and acceptor, unlike in the case of hole transfer to PTC-PTZ, a single linker-acceptor complex would not guarantee fast transfer, since its distance from the occupied trap would be random (unless the presence of the anchoring group may somehow *activate* the traps in its vicinity, ensuring the presence of a trapped electron in its close proximity). Assuming a uniform distribution of both traps and linkers on the NC surface, and considering that efficient transfer times of the order of 10 ps or less are achieved for a distance of less than 0.7 nm between anchoring group and electron trap (see Fig. 5), we estimate that a minimum of 5 acceptors would be needed in order to ensure a fast electron extraction. This number is compatible with the experimental estimate[4] of an average of 10 quinones required to achieve 98.7% quenching efficiency (i.e., efficient electron transfer to the acceptor).

In summary, we presented an atomistic study of photoexcited hole and electron transfer

from NC cores to molecular acceptors connected to the surface by either charge-delocalizing or charge-confining linkers. By describing these processes in terms of an Auger-mediated mechanism, we predicted huge differences in efficiency between transfers involving charge-delocalizing linkers (which can be as fast as hundreds of femtoseconds, in agreement with recent observations in CdS-PTC-PTZ conjugates), and those involving charge-confining linkers (where the fastest calculated transfer times are in the nanosecond range). In order to reconcile the latter slow processes with recent observations of a ps-fast electron transfer to quinone molecules in CdTe-based NCs, following the suggestion of the authors of that work, we assumed a surface-electron-trap-mediated transfer, recovering short lifetimes, consistent with experiment. The level of localization of the initial state constitutes the main difference between (a) hole transfer from core-delocalized states to PTC-PTZ acceptor states, and (b) electron transfer from surface-localized trap states to quinone acceptor, leading to three main consequences: (i) Whereas in (a) the dielectric environment of the CQD-acceptor conjugate (i.e., the solvent in which the nanostructures are dispersed) can be used as a mean by which the hole transfer time can be further fine tuned within a window of a few orders of magnitude, for the same choice of linker-acceptor complex, its effect is much reduced in (b), where the largest difference in the transfer time we find is less than a factor of 10 (for a dielectric constant variation from 2.2 to 8.5) - this is due to the fact that in the latter case both initial and final electronic states are on or outside the surface and therefore experience the same environment; (ii) the qualitative behavior of the transfer times as a function of the depth of the acceptor state, ΔE, is different in the two cases due to the different density of (final) states in conduction and valence band; (iii) as, unlike in (a), in (b) the transfer time depends crucially on the distance between trap and acceptor, several linker-acceptor complexes are required to guarantee fast transfer in (b), whereas sub-ps transfer times are achievable in (a) with a single linker-acceptor.

These results further confirm that (1) AMT can (i) explain charge transfer to molecular acceptor-linker complexes and (ii) accurately reproduce its observed rates; (2) Auger-

mediated processes are ubiquitous and extremely efficient in semiconductor NCs, and are responsible for any fast charge transfer mechanism, whether to surface traps,[8,10] to intrinsic defects, such as impurity states,[9] or to molecular acceptors, positioned either directly on the dot surface[15] or, as in the present case, linked to it via a ligand molecule.

Acknowledgement

M.C. gratefully acknowledges financial support from the School of Electronic and Electrical Engineering.

Supporting Information Available

Comparison between the charge densities calculated for hole-deconfining (HD) and hole-non-deconfining (HND) linkers, Calculated Auger-mediated hole transfer times in a CdSe NC with four PTC/PTZ conjugates, Charge density in the presence of an electron-non-deconfining (END) linker, AMeT times from a core electron, AMeT times from a surface-trapped electron

References

(1) Kovalenko, M. V.; Manna, L.; Cabot, A.; Hens, Z.; Talapin, D. V.; Kagan, C. R.; Klimov, V. I.; Rogach, A. L.; Reiss, P.; Milliron, D. J. *et al.* Prospects of Nanoscience with Nanocrystals. *ACS Nano* **2015**, *9*, 1012-1057.

(2) Sigaeva, A; Ong. Y; Damle, V. G.; Morita, A.; van der Laan, K. J.; Schirhagl. R. Optical Detection of Intracellular Quantities Using Nanoscale Technologies. *Acc. Chem. Res.* **2019**, *52*, 1739-1749.

(3) Hu, J.; Liu, M.-h.; Zhang, C.-y. Construction of Tetrahedral DNA-Quantum Dot Nanos-

tructure with the Integration of Multistep Förster Resonance Energy Transfer for Multiplex Enzymes Assay. *ACS Nano*, **2019**, *13*, 7191-7201.

(4) Harvie, A. J.; Smith, C. T.; Ahumada-Lazo, R.; Jeuken, A. J. C.; Califano, M.; Bon, R. S.; Hardman, S. J. O.; Binks, D. J.; Critchley, K. Ultrafast Trap State-Mediated Electron Transfer for Quantum Dot Redox Sensing.*J. Phys. Chem. C* **2018**, *122*, 10173-10180.

(5) Huang, Z.; Xu, Z.; Mahboub, M.; Liang, Z.; Jaimes, P.; Xia, P.; Graham, K. R.; Tang, M. L.; Lian, T. Enhanced Near-Infrared-to-Visible Upconversion by Synthetic Control of PbS Nanocrystal Triplet Photosensitizers. *J. Am. Chem. Soc.*, **2019**, *141*, 9769-9772.

(6) Lian, S.; Weinberg, D. J.; Harris, R. D.; Kodaimati, M. S.; Weiss, E. A. Subpicosecond Photoinduced Hole Transfer from a CdS Quantum Dot to a Molecular Acceptor Bound Through an Exciton-Delocalizing Ligand *ACS Nano* **2016**, *10*, 6372-6382.

(7) Frantsuzov, P. A.; Marcus, R. A. Explanation of Quantum Dot Blinking Without the Long-Lived Trap Hypothesis. *Phys. Rev. B* **2005**, *72*, 155321.

(8) Gomez-Campos, F. M.; Califano, M. Hole Surface Trapping in CdSe Nanocrystals: Dynamics, Rate Fluctuations, and Implications for Blinking. *Nano Lett.* **2012**, *12*, 4508-4517.

(9) Califano, M.; Gomez-Campos, F. M. Universal Trapping Mechanism in Semiconductor Nanocrystals. *Nano Lett.* **2013**, *13*, 2047-2052.

(10) Califano, M. Origins of Photoluminescence Decay Kinetics in CdTe Colloidal Quantum Dots. *ACS Nano* **2015**, *9*, 2960-2967.

(11) Wang, L.-W.; Zunger, A. Local-Density-Derived Semiempirical Pseudopotentials. *Phys. Rev. B* **1995**, *51*, 17398-17416.

(12) Kilina, S.; Ivanov, S.; Tretiak, S. Effect of Surface Ligands on Optical and Electronic Spectra of Semiconductor Nanoclusters. *J. Am. Chem. Soc.* **2009**, *131*, 7717-7726.

(13) Wang, L.-W.; Zunger, A. Pseudopotential Calculations of Nanoscale CdSe Quantum Dots. *Phys. Rev. B* **1996**, *53*, 9579-9582.

(14) Graf, P. A.; Kim, K.; Jones, W. B.; Wang, L.-W. Surface Passivation Optimization Using DIRECT *J. Comput. Phys.*, **2007**, *224*, 824-835.

(15) Zhu, H.; Yang, Y.; Hyeon-Deuk, K.; Califano, M.; Song, N.; Wang, Y.; Zhang, W.; Prezhdo, O. V.; Lian, T. Auger-Assisted Electron Transfer from Photoexcited Semiconductor Quantum Dots. *Nano Lett.* **2014**, *14*,1263-1269

(16) Franceschetti, A.; Fu, H.; Wang, L.-W. & Zunger, A. Many-Body Pseudopotential Theory of Excitons in InP and CdSe Quantum Dots. *Phys. Rev. B* **1999**, *60*, 1819-1829.

(17) Wang, L.-W.; Califano, M.; Zunger, A.; Franceschetti, A. Pseudopotential Theory of Auger Processes in CdSe Quantum Dots. *Phys. Rev. Lett.* **2003**, *91*, 056404.

(18) Frederick, M. T.; Weiss, E. A. Relaxation of Exciton Confinement in CdSe Quantum Dots by Modification with a Conjugated Dithiocarbamate Ligand *ACS Nano* **2010**, *6*, 3195-3200.

(19) Azpiroz, J. M.; De Angelis, F. Ligand Induced Spectral Changes in CdSe Quantum Dots. *ACS Appl. Mater. Interfaces* **2015**, *7*, 19736-19745.

(20) Voznyy, O. Mobile Surface Traps in CdSe Nanocrystals with Carboxylic Acid Ligands. *J. Phys. Chem. C* **2011**, *115*, 15927-15932.

(21) Koposov, A. Y.; Cardolaccia, T.; Albert, V.; Badaeva, E.; Kilina, S.; Meyer, T. J.; Tretiak, S.; Sykora, M. Formation of Assemblies Comprising Ru-Polypyridine Complexes

and CdSe Nanocrystals Studied by ATR-FTIR Spectroscopy and DFT Modeling *Langmuir* **2011**, *27*, 8377-8383.